

Distinct MicroRNA Expression Profile and Targeted Biological Pathways in Functional Myeloid-derived Suppressor Cells Induced by Δ^9 -Tetrahydrocannabinol *in Vivo*

REGULATION OF CCAAT/ENHANCER-BINDING PROTEIN α BY MicroRNA-690^{*§}

Received for publication, July 19, 2013, and in revised form, November 6, 2013. Published, JBC Papers in Press, November 7, 2013, DOI 10.1074/jbc.M113.503037

Venkatesh L. Hegde, Sunil Tomar, Austin Jackson, Roshni Rao, Xiaoming Yang, Udai P. Singh, Narendra P. Singh, Prakash S. Nagarkatti, and Mitzi Nagarkatti¹

From the Department of Pathology, Microbiology and Immunology, University of South Carolina School of Medicine, Columbia, South Carolina 29208

Background: Cannabinoids induce potent myeloid-derived suppressor cells (MDSCs) *in vivo*.

Results: Functional MDSCs induced by THC show distinct miRNA expression patterns.

Conclusion: Specific miRNA may play important roles in MDSC development and function by regulating target genes involved in myeloid cell differentiation.

Significance: Select miRNA could be important molecular targets to manipulate MDSC activity in cancer and inflammatory diseases.

Δ^9 -Tetrahydrocannabinol (THC), the major bioactive component of marijuana, has been shown to induce functional myeloid-derived suppressor cells (MDSCs) *in vivo*. Here, we studied the involvement of microRNA (miRNA) in this process. CD11b⁺Gr-1⁺ MDSCs were purified from peritoneal exudates of mice administered with THC and used for genome-wide miRNA profiling. Expression of CD31 and Ki-67 confirmed that the THC-MDSCs were immature and proliferating. THC-induced MDSCs exhibited distinct miRNA expression signature relative to various myeloid cells and BM precursors. We identified 13 differentially expressed (>2-fold) miRNA in THC-MDSCs relative to control BM precursors. *In silico* target prediction for these miRNA and pathway analysis using multiple bioinformatics tools revealed significant overrepresentation of Gene Ontology clusters within hematopoiesis, myeloid cell differentiation, and regulation categories. Insulin-like growth factor 1 signaling involved in cell growth and proliferation, and myeloid differentiation pathways were among the most significantly enriched canonical pathways. Among the differentially expressed, miRNA-690 was highly overexpressed in THC-MDSCs (~16-fold). Transcription factor CCAAT/enhancer-binding protein α (C/EBP α) was identified as a potential functional target of miR-690. Supporting this, C/EBP α expression was attenuated in THC-MDSCs as compared with BM precursors and exhibited an inverse relation with miR-690. miR-690 knockdown using peptide nucleic acid-antagomiR was able to unblock and significantly increase C/EBP α expression establishing the functional link. Further, CD11b⁺Ly6G⁺Ly6C⁺ and CD11b⁺Ly6G⁻Ly6C⁺ purified subtypes showed high levels of miR-690 with atten-

uated C/EBP α expression. Moreover, EL-4 tumor-elicited MDSCs showed increased miR-690 expression. In conclusion, miRNA are significantly altered during the generation of functional MDSC from BM. Select miRNA such as miR-690 targeting genes involved in myeloid expansion and differentiation likely play crucial roles in this process and therefore in cannabinoid-induced immunosuppression.

Mature microRNA (miRNA)² are a class of small (19–25 nucleotides), single-stranded, noncoding RNAs that play a crucial role in gene regulation. miRNA act as adaptors that guide RNA-induced gene silencing complex to target mRNAs by complementary base pairing, primarily within the 3'-UTR, which results in target gene silencing either by inhibition of translation or degradation of the mRNA, or both (1, 2). Although effective and functional target interaction does not require perfect complementarity between miRNA and mRNA sequences, a nearly perfect base pairing of a 7-nucleotide "seed sequence" at the 5' end (positions 2–8) of miRNA appears to be one of the key determinants of target recognition (2, 3). Most mammalian mRNAs are believed to be conserved targets of miRNA (4). The pattern of miRNA expression is organ- and cell type-specific, and significant changes in their expression are associated with processes such as cancer, inflammation, and infectious diseases in mice and humans (1, 5).

miRNA regulate several aspects of the immune system. They influence various innate and acquired immunological processes (6–8). Significant changes in miRNA expression have been

* This work was supported, in whole or in part, by National Institutes of Health Grants P01AT003961, P2ORR032684, R01AT006888, R01ES019313, and R01MH094755. This work was also supported by Veterans Affairs Merit Award 1 01BX001357 (to P. S. N. and M. N.).

§ This article contains supplemental Tables S1 and S2.

¹ To whom correspondence should be addressed: 6439 Garner's Ferry Rd., Bldg. 1, Rm. C27, Columbia, SC 29209. Tel.: 803-216-3404; Fax: 803-216-3413; E-mail: mnagark@usmed.sc.edu.

² The abbreviations used are: miR/miRNA, microRNA(s); C/EBP α or Cebp α , CCAAT/enhancer-binding protein α ; GO, Gene Ontology; MDSC, myeloid-derived suppressor cell; THC, Δ^9 -tetrahydrocannabinol; qPCR, quantitative PCR; IGF, insulin-like growth factor; PNA, peptide nucleic acid; PE, phycoerythrin; G-CSF, granulocyte colony-stimulating factor; GM-CSF, granulocyte/macrophage colony-stimulating factor; IPA, Ingenuity pathway analysis; BM, bone marrow.

observed during cell development and differentiation (8–10). Genome-wide analysis of miRNA expression has been performed for various immune cell types such as mouse lymphocyte subsets (11) and human B and T lymphocytes (5, 9, 11). Moreover, unique miRNA expression profiles are known to be associated with immune cells or their differentiation states (10, 12).

Myeloid-derived suppressor cells (MDSCs) are defined by their myeloid origin, immature state, and potent T cell-suppressive function. In mice, MDSC population are commonly identified by CD11b⁺ and Gr-1⁺ expression and T cell-suppressive activity (13–15). MDSCs are believed to regulate immune responses in normal state as well as during inflammation, infection, and cancer (15–18). MDSCs can potently suppress cytotoxic activities of natural killer (NK) and NKT cells, as well as the adaptive immune response mediated by CD4⁺/CD8⁺ T cells. MDSCs use multiple pathways to dampen T cell activity including production of arginase 1 and up-regulation of nitric-oxide synthase 2. Arginase 1 and nitric-oxide synthase 2 metabolize L-arginine needed for T cells and thereby block translation of the T cell CD3 zeta chain, inhibit T cell proliferation, and promote T cell apoptosis. In addition, MDSCs can also secrete immunosuppressive cytokines and induce regulatory T cell development in certain cases.

MDSCs are induced rapidly in various pathological conditions mainly infections, inflammatory diseases, and cancer. They accumulate in the blood, bone marrow, and secondary lymphoid organs of tumor-bearing mice and play an important role in causing immune suppression and tumor evasion. Although it is evident that MDSCs may serve as potential therapeutic targets to promote anti-tumor immune responses or to inhibit inflammatory responses such as in the case of autoimmune disease or during transplant rejection, further characterization is necessary with respect to molecular markers and pathways to determine how functional MDSCs develop and accumulate.

Our recent studies have explored the mechanism of immune regulation by several natural compounds such as cannabinoids and resveratrol involving induction of MDSCs (19–23). We made an exciting observation that activation of cannabinoid receptors by immunosuppressive, natural cannabinoids from marijuana such as THC lead to robust induction of functional MDSCs in mice (22). To understand the nature and origin of THC-induced functional MDSCs, in this study, we sought to explore the miRNA expression so as to identify cell type-specific miRNA pertaining to MDSCs and their target pathways. To this end, we performed a genome-wide analysis of miRNA expression by microarray-based profiling in highly immunosuppressive CD11b⁺Gr-1⁺ MDSCs induced by THC *in vivo*, relative to control CD11b⁺Gr-1⁺ precursor cells from naïve bone marrow, as well as various other myeloid cells from the periphery. We identified differentially expressed miRNA unique to functional MDSCs induced by THC. Further, highly predictive target genes and putative pathways were analyzed using the latest genomics and bioinformatics computational tools. One of the highest differentially expressed miRNA in functional MDSC, miR-690, was further explored with respect to regulation of target transcription factor and myeloid regulator C/EBP α .

EXPERIMENTAL PROCEDURES

Reagents—THC was provided by the National Institute on Drug Abuse, National Institutes of Health (Rockville, MD). THC was initially dissolved in Me₂SO and diluted in sterile PBS for injections. The mAbs, FITC-conjugated anti-CD11b, phycoerythrin (PE)-conjugated anti-Gr-1 (clone RB6–8C5), PE anti-Ly6-G (clone IA-8), PE anti-CD11c, PE-Cy7 anti-Ly6-C (clone HK1.4), PE anti-F4/80, PE anti-Ki67, PE anti-CD31, and purified mouse Fc block (anti-CD16/CD32) were purchased from BioLegend. Anti-CD11b and anti-PE microbeads, magnetic sorting columns, and equipment were from Miltenyi Biotech. [³H]Thymidine was purchased from GE Healthcare. Mouse G-CSF and GM-CSF were from R&D Systems. Red blood cell lysis buffer and all other chemicals and reagents were from Sigma-Aldrich or Invitrogen.

Mice—Adult female C57BL/6 (WT) mice, 8–10 weeks of age, were procured from the National Cancer Institute, National Institutes of Health (Frederick, MD). The mice were maintained under typical pathogen-free conditions in the animal resource facility of the University of South Carolina School of Medicine. All experiments and procedures were authorized by the Institutional Animal Care and Use Committee.

Cells—The mice were injected with THC (25 mg/kg) intraperitoneally to induce MDSCs as described previously (22). After 16 h, infiltrating cells in the peritoneal cavity were harvested by performing lavage with sterile, ice-cold PBS (5 ml \times 3). The cells were spun down and reconstituted in FACS buffer (PBS + 2% FBS) for immunostaining and flow cytometry. CD11b⁺Gr-1⁺ MDSCs were purified to ~93% by FACS sorting (FACS AriaTM; Becton Dickinson). T cell-suppressive activity of THC-MDSC were confirmed by a standard T cell proliferation assay as described previously (22). CD11b⁺Ly6-G⁺Ly6C⁺ granulocytic and CD11b⁺Ly6-G⁻Ly6C⁺ monocytic subsets were purified by FACS sorting to >96% purity. Various control myeloid cells were purified to >90% purity either by immunomagnetic separation (Miltenyi Biotech) or FACS sorting (19, 21–23). Briefly, naïve splenocytes were obtained from WT mice after preparing a single cell suspension of the spleen followed by RBC lysis. Bone marrow cells naïve WT mice were prepared by flushing tibia with ice-cold PBS followed by RBC lysis (22). Naïve spleen CD11b⁺Gr-1⁺ cells (control SPL-MDSC) and CD11b⁺Gr-1⁺ precursors from naïve BM (control BM MDSC precursors) were purified by immunolabeling and FACS sorting. Naïve spleen dendritic cells were sorted following labeling with anti-CD11c-PE antibody. Control spleen CD11b⁺Gr-1⁻ macrophages were purified by a two-step magnetic bead isolation-positive selection with CD11b microbeads followed by negative selection using anti-Gr-1-PE antibody and anti-PE microbeads. CD11b⁺Gr-1⁺ tumor-induced MDSC were purified from spleens of BL/6 tumor-bearing mice on day 12 following inoculation with EL-4 tumor cells. All sorted cells were tested for purity (>90%) by flow cytometry before total RNA isolation.

Total RNA Extraction—Total RNA including small RNAs were extracted using QIAzol lysis reagent and a miRNeasy mini kit (Qiagen) according to the manufacturer's instructions. The concentration of RNA was determined using a spectrophotom-

miRNA Expression Profiling of THC-induced Functional MDSCs

eter, and the RNA integrity was verified using Agilent 2100 BioAnalyzer (Agilent Tech, Palo Alto, CA). Total RNA from PNA-anti-miR transfection experiments were extracted using RNAqueous® phenol-free total RNA extraction kit (Ambion) as recommended.

miRNA Expression Profiling: Labeling and Hybridization—The Affymetrix GeneChip® miRNA 1.0 array platform described previously (24) was used for profiling miRNA expression as per the manufacturer's instructions. The array included oligonucleotide probe sets for 609 mouse miRNA from Sanger miRBase (v11) (25) with multiple probes for each mature miRNA sequence. Total RNA containing small RNA were labeled with biotin using FlashTag Biotin HSR RNA labeling kit (Genisphere, Hatfield, PA). Pre-labeled spike control oligonucleotides were spiked in to the controls used for labeling and hybridization, as well as for data normalization purposes. The hybridization mixture contained premixed hybridization controls (bioB, bioC, bioD, and cre). Each labeled sample was hybridized to the array at 48 °C and 60 rpm for 16 h, then washed, and stained with fluorescent-conjugated streptavidin on a Fluidics Station. The stained chip was washed and scanned on GeneChip Scanner (Affymetrix) to generate the chip image and the data file. Total RNA isolated from three independent cell sorts for THC-induced MDSCs and control BM MDSC precursors and two independent cell sorts for control spleen MDSCs, control spleen macrophages, and control spleen dendritic cells were pooled before high throughput analysis. Each cell sort represents cells obtained and purified from three to five mice. These samples were analyzed separately in real time qPCR validation.

Data Handling—The microarray image data were analyzed using Affymetrix miRNA QC Tool software for data summarization, normalization, and quality control. Hybridization signals that showed aberrant properties and were <3 standard deviations over the mean background value were excluded. Statistical significance (*p* values) for “detection calls” were determined by Affymetrix test. Probe sets with a *p* value lower than 0.05 were called present (true). The log-transformed fluorescence intensity values were mean-centered and visualized by heat maps. Comparisons were made between miRNA expression profile for THC-MDSC and control BM precursors and other control myeloid cells from naïve WT mice. The miRNA that showed >2-fold higher or lower values in THC-MDSC were considered as differentially expressed. Fold change heat maps, Venn diagrams, and scatter plots were further used for differential expression analysis and visualization.

Real Time qPCR—Several miRNA were validated by real time qPCR assays. Total RNA were reverse transcribed to obtain cDNA using miScript kit (Qiagen). For the detection of mature miRNA: mmu-miR-22, mmu-miR-20a, mmu-miR-15b, mmu-miR-335-5p, and control RNU_1A, qPCR was performed using miScript primer assays containing specific forward primer and a universal reverse primer and QuantiTect SYBR Green PCR master mix (Qiagen) using StepOne real time PCR thermal cycler (Applied Bio). For mmu-miR-690 and internal control U6, primer sets were obtained from Applied Biological Materials Inc. (Richmond, Canada). Relative quantification was calculated by $2^{(-\Delta\Delta Cq)}$ method and expressed relative to endogenous

TABLE 1
Real time qPCR primers used in the study

Gene	Primer	Sequence (5' → 3')
<i>Cebpa</i>	Cebpa-F	CAA GAA CAG CAA CGA GTA CCG
	Cebpa-R	GTC ACT GGT CAA CTC CAG CAC
<i>Nedd4</i>	Nedd4-F	TTC GAG GAC GAG GTA TGG G
	Nedd4-R	GGT ACG GAT CAG CAG TGA ACA
<i>Ptpn11</i>	Ptpn11-F	ATG ACA TCG CGG AGA TGG TTT
	Ptpn11-R	GGG TTA CTC TTA CTG GGC CTT
<i>Runx1</i>	Runx1-F	GCA GGC AAC GAT GAA AAC TAC T
	Runx1-R	GCA ACT TGT GGC GGA TTT GTA
<i>E2f1</i>	E2f1-F	CTC GAC TCC TCG CAG ATC G
	E2f1-R	GAT CCA GCC TCC GTT TCA CC
<i>Rn18s</i>	18S-F	GCC CGA GCC GCC TGG ATA C
	18S-R	CCG GCG GGT CAT GGG AAT AAC

controls RNU_1A or U6. Total RNA isolated from two or three independent cell sorts from three to five mice per sample obtained as mentioned above were analyzed separately in this assay to obtain standard deviation. Relative quantification values were compared using Student's *t* test. Real time qPCR primers for *Cebpa* and other target genes were synthesized from IDT DNA Technologies (Table 1).

Computational Analysis of miRNA Targets and Pathways: miRNA Target Prediction—We analyzed differentially expressed miRNA in THC-MDSC versus BM precursors *in silico* for their target genes. We used TargetScan, version 5.1 (2, 4), RNAhybrid (v2.1) (26), and miRanda (27) miRNA algorithms via miRWalk suite (28). We restricted our searches to minimum miRNA seed length of 7 nucleotides and binding sites on the 3'-UTR of target mRNA. Probability distribution of random matches was set at 0.05 (Poisson *p* value). Targets with *p* ≤ 0.05 and predicted by at least two of the three algorithms were identified as predicted targets. For experimentally supported targets curated from the literature, we used miRecords (29) and the latest version of TarBase 6.0 (30).

Pathway Analysis—Ingenuity pathway analysis (IPA) software (Ingenuity® Systems) was used to identify the molecular and functional annotations and canonical biological pathways potentially influenced by target genes of differentially expressed miRNA. Significant enrichment of target genes into functional annotation categories was determined and ranked based on (i) the ratio of the number of molecules from the data set that map to the annotation category divided by the total number of molecules associated with the category and (ii) the *p* value from the right-tailed Fisher's exact test representing the probability that the association between the genes in the data set and the annotation is due to chance alone. Similarly, pathway analysis was performed using IPA to identify the significantly enriched canonical pathways most relevant to the target gene data set from the IPA pathway library sourced from the Kyoto Encyclopedia of Genes and Genomes (31).

Gene Ontology Mapping—Gene Ontology (GO) enrichment analysis and mapping of miRNA target genes was performed using Cytoscape suite, an open source bioinformatics platform for analyzing and visualizing complex networks (32) equipped with ClueGo and CluePedia plugins (33).

PNA-miRNA Inhibitors—PNA anti-miRs against the mature form of mmu-miR-690 were synthesized by PNABio (Thousand Oaks, CA). A scrambled sequence PNA anti-miR was used as the negative control. In addition, we used a fluorescently

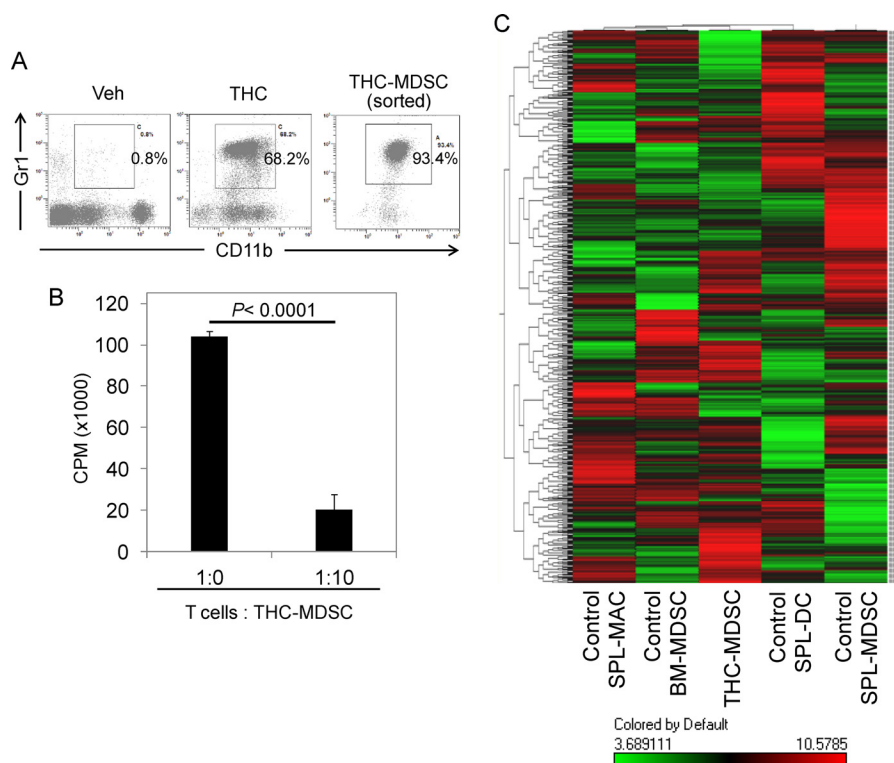


FIGURE 1. miRNA expression profiling of THC-induced functional MDSCs. *A*, flow cytometric analysis of cells harvested from peritonea of mice, 16 h after *in vivo* administration of THC or vehicle (*Veh*) showing robust induction of CD11b⁺Gr-1⁺ MDSCs. THC-induced MDSCs were sorted to >93% purity. *B*, purified THC-MDSCs co-cultured with syngenic T cells polyclonally stimulated with concanavalin A showing significant T cell-suppressive activity as determined by thymidine incorporation. *C*, false color dendrogram representing unsupervised hierarchical clustering of relative expression values for mouse miRNA in purified cell types as indicated determined using Affymetrix GeneChip miRNA array shows distinct signature in THC-induced MDSCs. Mean expression values were log-transformed and mean-centered. Each sample column represents data from total RNA pooled from two to three independent cell sorts using groups of up to five mice each. In the *color scale*, red denotes expression above mean, and green denotes expression below mean. *SPL*, spleen; *MAC*, macrophage; *DC*, dendritic cell.

conjugated (5-FAMTM, green fluorescence) negative control PNA to check transfection efficiency and optimize the transfection.

Transfection and Knockdown of miR-690—THC-induced MDSCs obtained from the peritoneum of mice were plated in DMEM without antibiotics and containing 10 ng/ml GM-CSF and 50 ng/ml G-CSF. PNA inhibitors were suspended in nuclease-free water and completely dissolved by heating to 60 °C for 5–10 min. PNA inhibitors contain a conjugated cell-penetrating peptide and can be used without a transfection reagent; however, transfection reagent could be added to further facilitate cell penetration. For the primary MDSCs, we optimized and used a transfection mixture containing control or miR-690 PNA anti-miR to a final concentration of 0.5 μM with a low concentration of Lipofectamine 2000 (0.2 μl; 0.04% final concentration). Cells were supplemented with complete medium after 12 h and harvested after 24 h. Total RNA and protein were extracted for analysis.

Western Blotting—Protein extracts (~20 μg) were separated by 10% polyacrylamide gel electrophoresis containing 0.1% SDS and transferred to nitrocellulose membrane. The membranes were probed with antibodies against C/EBPα or control β-actin (Santa Cruz Biotechnology). Blots were developed with HRP-conjugated secondary antibody and visualized using the ECL system (Pierce).

RESULTS

Functional CD11b⁺Gr-1⁺ MDSCs Exhibit Distinct miRNA Expression Profile—Although miRNA have been shown to play a critical role in the differentiation of myeloid cells, the global miRNA expression in MDSCs when compared with other myeloid populations, specifically to characterize cell type-specific miRNA, has not been performed. Administration of THC triggers massive induction of MDSCs (22). We therefore sought to determine and compare the miRNA expression of these MDSCs with other cells. We administered THC into C57BL/6 (WT) mice to obtain large numbers of CD11b⁺Gr-1⁺ cells (Fig. 1A) in the peritoneal cavity as reported previously (22). The cells were further enriched by sorting to ~93% purity. We corroborated their immunosuppressive functions, by testing their ability to suppress T cell proliferation (Fig. 1B). To compare THC-induced MDSCs with other cell types, we used the following cells: normal CD11b⁺Gr-1⁺ cells (control BM-MDSC precursors) purified from the bone marrow; normal splenic MDSCs (CD11b⁺Gr-1⁺), normal splenic macrophages (Gr-1⁻CD11b^{high}), and normal splenic dendritic cells (CD11c⁺) all sorted from naïve WT mice with >90% purity.

Total RNA including small RNAs were isolated, and the miRNA transcript expression profile was determined using Affymetrix GeneChip[®] array. The array had 609 mouse miRNA

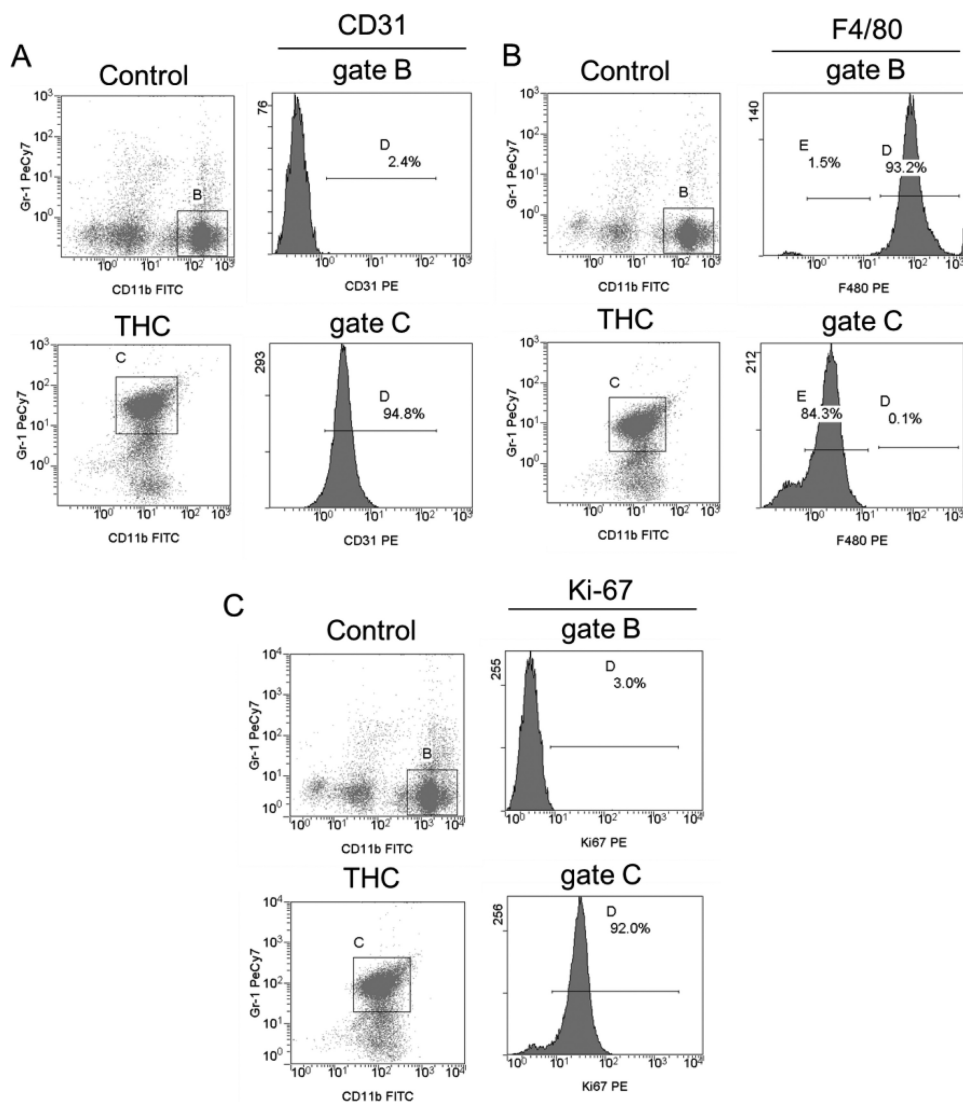


FIGURE 2. Analysis of immature, mature myeloid, and proliferation markers on THC-MDSC. Peritoneal cells harvested at 16 h from control and THC-injected mice were triple-stained for CD11b and Gr-1 along with CD31 (A), F4/80 (B), or Ki-67 (C) and analyzed by FACS. Expression of CD31 or F4/80 or Ki-67 (histograms) on gated CD11b^{high} classical mature macrophages from control peritoneum and CD11b⁺Gr-1⁺ MDSC from THC-treated mice is shown. A representative plot for each treatment is shown, and frequencies of gated population are indicated.

probes. The normalized relative expression values were analyzed by unsupervised hierarchical clustering and visualized in the form of dendrograms (Fig. 1C). THC-induced functional MDSCs showed distinct miRNA expression profile as compared with control BM-MDSC precursors (BM-MDSC) from naïve mice. miRNA expression profile of THC-MDSCs was also distinctly different from that of control spleen MDSCs, CD11b⁺(Gr-1⁻) mature macrophages, and CD11c⁺ dendritic cells, all obtained from spleens of WT mice.

THC-induced MDSC have been characterized as immature myeloid cells derived from BM that have attained a potent immunosuppressive phenotype (22). To further corroborate this, we tested these cells for the expression of immature myeloid marker CD31. The majority of CD11b⁺Gr-1⁺ MDSCs induced by THC expressed CD31 (Fig. 2A). In comparison, the classical, CD11b^{high} mature macrophages from control peritoneum did not express CD31. Further, gated THC-MDSCs showed relatively low expression of F4/80 when compared to CD11b^{high} macrophages (Fig. 2B). Intranuclear staining for

Ki-67 revealed that ~92% of THC-induced MDSCs were undergoing proliferation at 16 h after THC injection (Fig. 2C). These data further confirmed the immature nature of THC-induced MDSCs and ruled out the possibility that they may consist of reprogrammed mature myeloid cells.

Correlation scatter plots of miRNA expression values between THC-induced functional MDSC and various control myeloid cells are shown in Fig. 3. The R^2 values highlight the difference in miRNA expression of THC-MDSCs compared with control myeloid cells. As shown, miRNA expression of THC-MDSCs was found to be highly distinct compared with control dendritic cells ($R^2 = 0.4736$) and was much closer to control BM-MDSC precursors ($R^2 = 0.8505$).

Differentially Expressed miRNA in Functional CD11b⁺Gr-1⁺ MDSCs—We compared the level of expression of miRNA in THC-MDSCs relative to control MDSCs and other myeloid cells. A large number of miRNA among the 609 mouse miRNA analyzed were undetectable or were unchanged (<2-fold) in THC-MDSC compared with other samples. We identified dif-

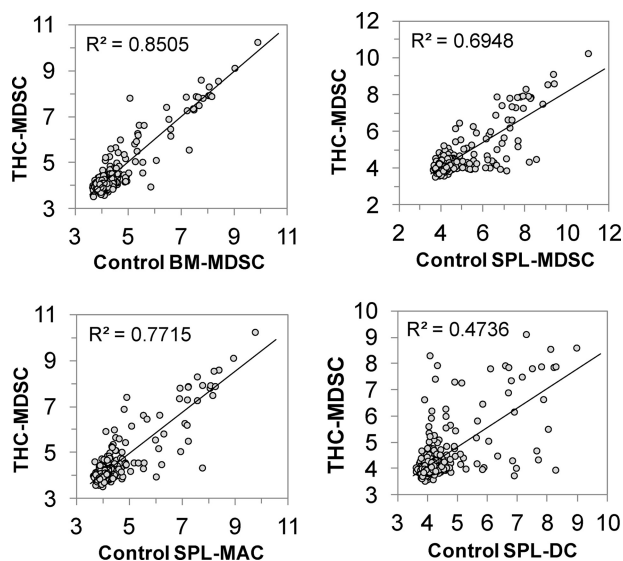


FIGURE 3. Pairwise correlation comparison of miRNA expression in THC-MDSC with other myeloid cells. Pearson correlation scatter plots of mouse miRNA log₂ expression values (signal intensity) for *in vivo* THC-induced MDSCs versus various control myeloid cells purified from naive mice. The R² coefficients for each comparison are shown.

ferentially expressed miRNA showing greater than 2-fold differences in expression in THC-MDSC. The number of miRNA that were overexpressed, unchanged, or underexpressed in THC-MDSCs for each comparison is represented in Venn diagrams (Fig. 4A). The heat map of differentially expressed miRNA in THC-MDSCs and their corresponding fold changes (Fig. 4B) indicates that a small number of miRNA were markedly altered in functional THC-induced MDSCs compared with their bone marrow precursors or other control myeloid cells.

Next, to investigate putative miRNA and their targets that may be potentially associated with the differentiation of BM precursors to immunosuppressive functional MDSCs *in vivo*, we focused on miRNA altered in THC-MDSCs relative to control BM-MDSC. A list of 13 differentially regulated miRNA (10 overexpressed and 3 underexpressed) with their seed sequences, chromosome locations, and miRBase accession numbers is shown in Table 2. mmu-miR-690 was the most highly overexpressed in THC-MDSC with a +6.7-fold difference, and mmu-miR-762 was the highly underexpressed with a -3.7-fold difference in expression. We validated some of the differentially expressed miRNA in THC-MDSC using real time qPCR. As shown in Fig. 4C, mmu-miR-15b, mmu-miR-20a, and mmu-miR-22 were significantly overexpressed, whereas mmu-miR-335-5p was significantly underexpressed in THC-MDSCs relative to control BM-MDSCs, which corroborated the overall trend observed with the high throughput array results.

Predicted Targets of Differentially Expressed miRNA in Functional MDSCs—To identify putative target genes regulated by miRNA in functional MDSCs, we employed multiple computational prediction tools as described under “Experimental Procedures.” Targets of differentially expressed miRNA in THC-MDSC predicted by at least two of the three leading and reliable algorithms (TargetScan, RNAhybrid and miRanda) with a *p* value of <0.05 were identified as predicted targets (supplemental Table

S1). It should be noted that TargetScan predictions are based on sequence complementarity to target sites with an emphasis on base pairing in the seed region as well as target mRNA UTR conservation (2, 3). RNAhybrid (26) is based on calculations of stability of secondary structures and energetically favorable hybridization between miRNA and target mRNA. miRanda with mirSVR scoring (27) uses weighted dynamic programming to compute optimal sequence complementarity and free energy (thermodynamic stability) of miRNA:mRNA duplex estimated by Vienna package as the secondary filter. Thus a combination of these tools provides a robust approach to identify high predictive, potential functionally relevant miRNA-target gene interactions. In addition to the conserved targets, this unique approach helps identify good targets that are poorly conserved, consistent with increasing experimental evidence supporting the fact that such interactions could also be functionally important (3, 34). Distribution of the number of targets predicted by the three software programs is represented in the form of a Venn diagram (Fig. 5A). A total of 12,815 genes were predicted by at least two of the three algorithms, among which 982 target genes were common to all three. Further, we used TarBase and miRecords databases and identified 21 experimentally supported targets for six of the differentially expressed miRNA in THC-MDSC. The predicted and the experimentally validated targets were merged and used as a single data set for pathway analysis.

Functional Annotation Enrichment Analysis—The enrichment of target genes into major functional annotation categories with respective enrichment *p* values and a number of associated target molecules is shown in Fig. 5B. We observed that cellular growth and proliferation, cell death including cell survival, and cellular development including cell differentiation and maturation were the most highly enriched categories for the miRNA targets in THC-MDSC. In addition, hematopoiesis and cell migration, particularly immune cell trafficking, were significantly enriched as well. Highly significant association (*p* < 0.001) of a number of targets of differentially expressed miRNA in THC-MDSC versus BM precursors with these functional categories suggests that these functions are most likely influenced or regulated by miRNA altered during the development and differentiation of functional MDSCs from BM precursors.

GO Enrichment Mapping—Gene Ontology enrichment analysis of miRNA target genes in THC-MDSC was performed and mapped for biological process: GO:0002376 immune system process (Fig. 6). We found highly significant overrepresentation of immune response (GO:0006955) and hemopoiesis (GO:0030097) in the target genes, with corrected *p* values for false positive discovery being <0.0005. In addition, interestingly, we saw significant overrepresentation of myeloid cell differentiation (GO:0030099) and regulation of myeloid cell differentiation (GO:0045637) GO classifications (*p* < 0.05), suggesting the putative involvement and significance of differentially expressed miRNA in THC-MDSC in the regulation of target genes associated with these processes.

miRNA Target Pathways in Functional MDSC—The predicted and experimentally supported target genes of differentially expressed miRNA in THC-MDSC were combined and analyzed for their significant association with canonical path-

miRNA Expression Profiling of THC-induced Functional MDSCs

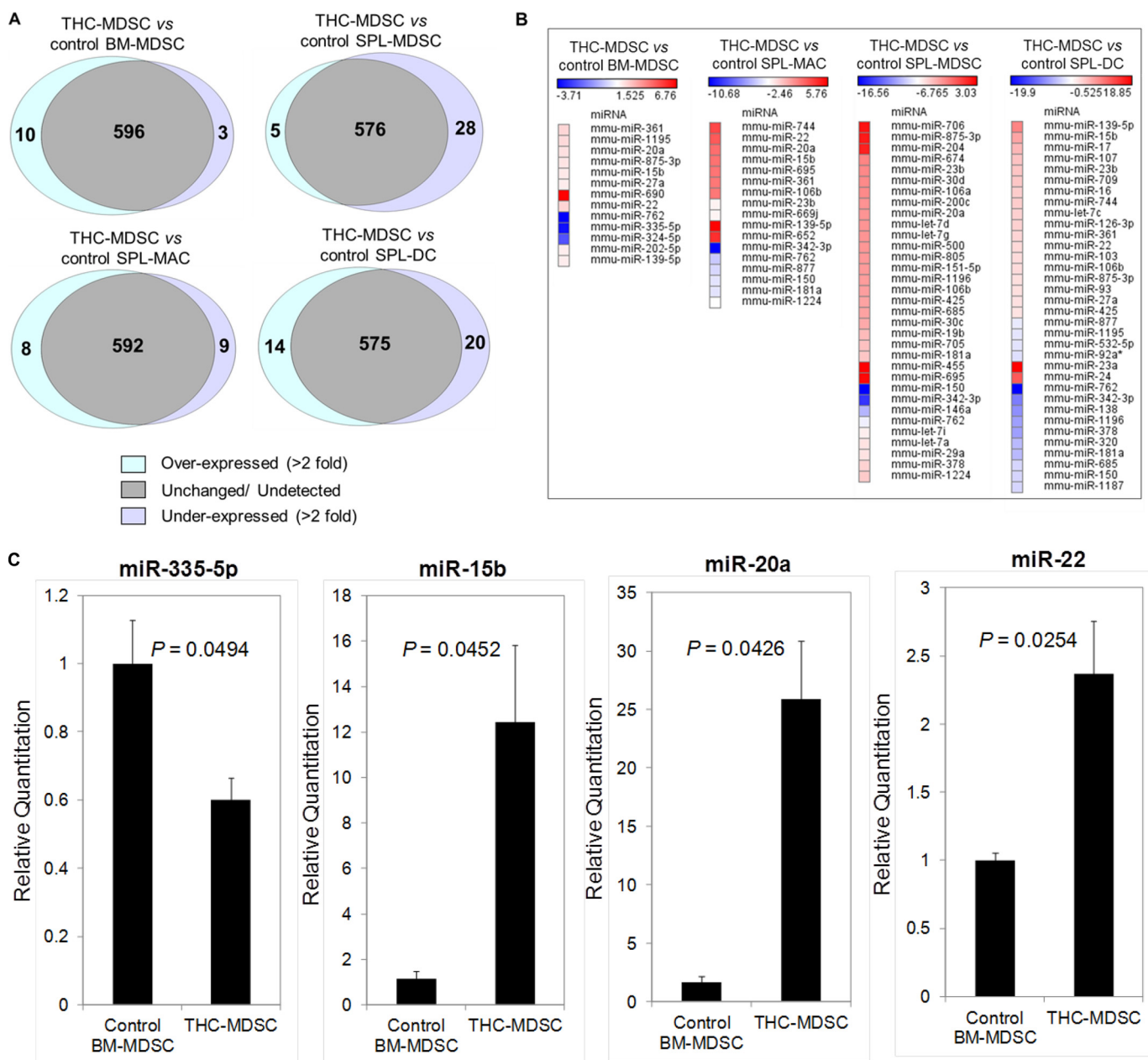


FIGURE 4. Differential expression of miRNA in THC-induced functional MDSCs. *A*, Venn diagrams representing number of up-regulated, down-regulated, and unchanged mouse miRNA in THC-MDSC compared with control myeloid cells as indicated. *B*, heat map of fold changes of differentially expressed miRNA in THC-MDSC showing >2-fold difference in expression as compared with control myeloid cells. *C*, real time qPCR validation. Total RNA from THC-MDSC and control BM-MDSC were analyzed for the indicated mouse miRNA expression by real time quantitative PCR normalized to internal control RNU-1A. Total RNA isolated from two or three independent cell sorts from groups of up to five mice for each sample were analyzed separately, and standard deviations are represented as *error bars*.

ways (supplemental Table S2). Several significantly predicted pathways appeared to be relevant to cell growth and proliferation in general, as well as development, differentiation, and function of myeloid cells. These molecular pathways were most likely to be influenced by the differentially regulated miRNA during the development and differentiation of BM precursors into functional MDSCs. Pathway maps for the top predicted pathways, (i) insulin-like growth factor 1 (Igf1) pathway (Fig. 7A), which regulates cell growth and proliferation in general, and (ii) multiple pathways involved in myeloid differentiation and function (Fig. 7B), are shown highlighting the target genes of overexpressed and under-expressed miRNA in THC-MDSC. Likely crucial transcription

factors and target molecules are listed in Table 3. Several important molecules in these pathways appear to be direct targets of differentially expressed miRNA in THC-MDSC, identifying multiple interesting miRNA-mediated regulatory nodes with likely roles in the differentiation of BM precursors into MDSCs and in the regulation of their expansion and function.

Experimental Validation of Predicted Target Genes—To test the biological relevance of these predictions, we determined the levels of some of the important predicted target gene transcripts in THC-MDSC by real time qPCR assays. Multiple up-regulated miRNA in THC-MDSC were found to target Nedd4 (Fig. 7A), which is a ubiquitin ligase known to regulate Igf1-Igf1r signaling.

TABLE 2

Differentially expressed (>2-fold) miRNA in THC-induced MDSC relative to control BM precursors

miRNA	Fold change	Chromosome location	Seed sequence ^a	miRBase accession number
Overexpressed				
mmu-miR-690	6.8	Chr16	AAGGCUA	MIMAT0003469
mmu-miR-22	2.5	Chr11	AGCUGCC	MIMAT0000531
mmu-miR-361	2.4	ChrX	UAUCAGA	MIMAT0000704
mmu-miR-1195	2.3	Chr17	GAGUUCG	MIMAT0005856
mmu-miR-20a	2.2	Chr14	AAAGUGC	MIMAT0000529
mmu-miR-875-3p	2.1	Chr15	CUGAAAA	MIMAT0004938
mmu-miR-15b	2.1	Chr3	AGCAGCA	MIMAT0000124
mmu-miR-27a	2.0	Chr8	UCACAGU	MIMAT0000537
mmu-miR-139-5p	2.0	Chr7	CUACAGU	MIMAT0000656
mmu-miR-202-5p	2.0	Chr7	UCCUAUG	MIMAT0004546
Underexpressed				
mmu-miR-324-5p	-2.0	Chr11	GCAUCCC	MIMAT0000555
mmu-miR-335-5p	-3.3	Chr6	CAAGAGC	MIMAT0000766
mmu-miR-762	-3.7	Chr7	GGGCUAG	MIMAT0003892

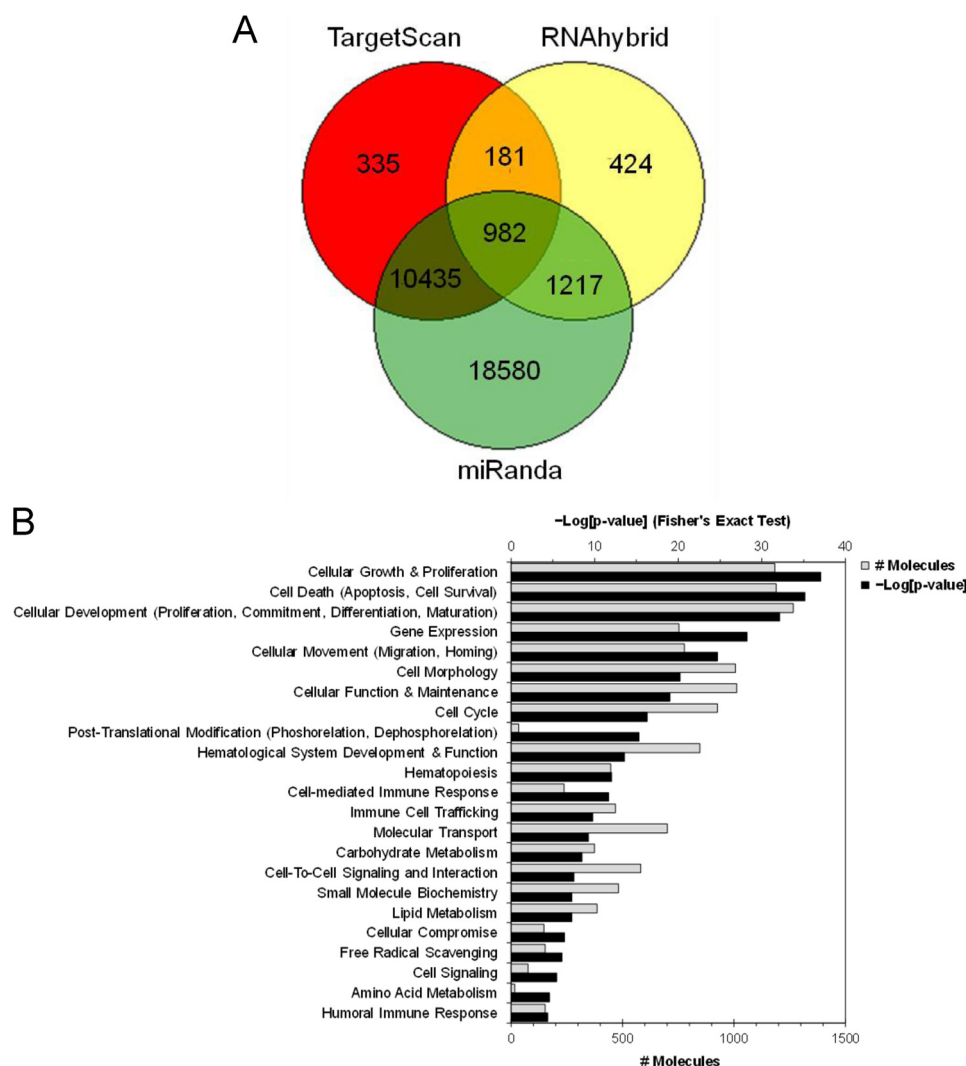
^a 7-mer seed sequence (bases 2–8).

FIGURE 5. miRNA target prediction and functional annotation analysis. *A*, Venn diagram showing distribution of number of gene targets for differentially expressed miRNA in THC-MDSC predicted by three algorithms as indicated. *B*, a combined set containing predicted and experimentally supported target genes for the differentially expressed miRNA in THC-MDSC were analyzed using Ingenuity[®] pathway analysis for significant enrichment of genes into functional annotation categories (Fisher's exact test *p* value). Significantly enriched categories excluding cancer and the neuronal annotations are shown with $-\log[p\text{-value}]$ and the number of miRNA gene targets.

Putative binding sites for miR-27a, miR-361, and miR-1195 on the 3'-UTR of Nedd4 mRNA are depicted in Fig. 8A. We found that Nedd4 mRNA levels were down-regulated in THC-MDSC relative to BM precursors by ~ 3 -fold (Fig. 8B).

Unlike Nedd4, protein-tyrosine phosphatase Ptpn11(SHP-2) involved in Igf1 signaling (Fig. 7A) was targeted by several up-regulated miRNA and miR-335-5p, which was down-regulated in THC-MDSC (Fig. 8C). Ptpn11 mRNA levels were signifi-

miRNA Expression Profiling of THC-induced Functional MDSCs

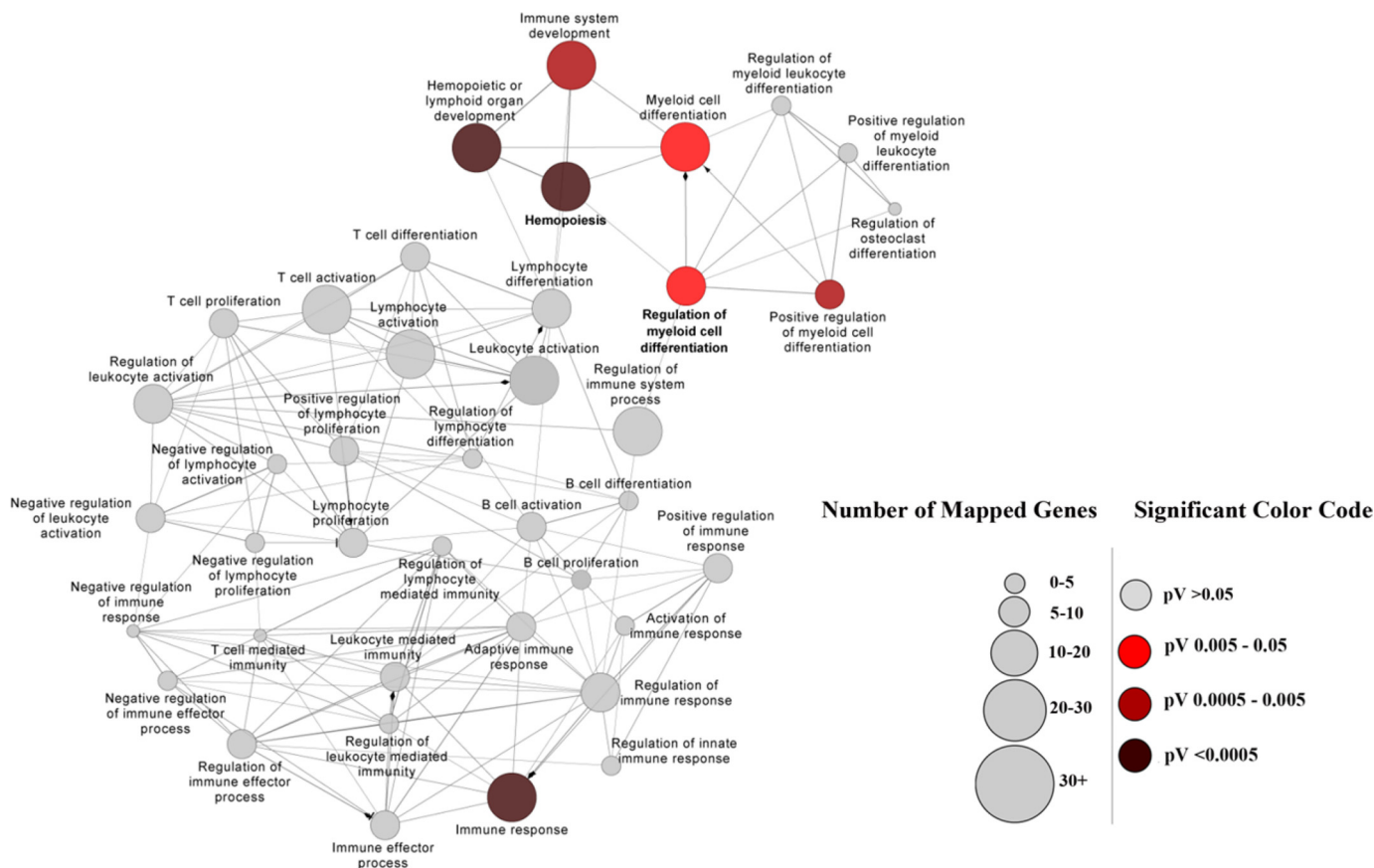


FIGURE 6. **GO enrichment mapping.** miRNA target genes in THC-MDSC were analyzed for GO enrichment and mapped for GO category: immune system process, using Cytoscape suite with ClueGo and CluePedia plugins. Two-sided hypergeometric statistic was performed with Kappa score threshold setting of 0.3. Enrichment and depletion were calculated based on Benjamini-Hochberg corrected p values (pV). GO clusters with enrichment p values > 0.05 and hence not significant are shown in gray. Significantly enriched GO groups with corrected p values of < 0.05 are denoted and color-coded for different significance levels as indicated. The diameter of each circle represents the number of miRNA target genes in each cluster scaled as shown.

cantly decreased in THC-MDSC compared with BM control (Fig. 8D).

Runx1-related transcription factor 1 (RUNX1), a regulator of normal hematopoiesis, plays an important role in myeloid differentiation (Fig. 7B). Target binding sites for multiple up-regulated and down-regulated miRNA in THC-MDSC were found on *Runx1* 3'-UTR (Fig. 8E). However, we observed a dramatic increase in the Runx1 transcript level in THC-MDSC over control precursors by close to 100-fold (Fig. 8F).

Transcription factor E2F1 is known to promote the expression of a number of miRNA including miR-27a and miR-22 that were up-regulated in THC-MDSC. When tested by qPCR, *E2f1* mRNA levels were significantly higher in THC-MDSC relative to BM controls (Fig. 8G).

Role of miR-690 in the Regulation of C/EBP α —miR-690 was the most highly overexpressed among altered miRNA in THC-MDSC over BM precursors (Table 2). The transcription factor C/EBP α is an important regulator of cell differentiation, particularly terminal differentiation of granulocytes. Interestingly, C/EBP α was one of the high predictive targets of miR-690 (Fig. 9A) based on multiple algorithms (miRanda-mirSVR and TargetScan). Validation by real time qPCR confirmed the significant up-regulation of miR-690 in THC-induced MDSC (Fig. 9B). *Cebpa* mRNA levels and protein expression were assessed by qPCR (Fig. 9C) and Western blotting (Fig. 9, D and E),

respectively. BM precursors showed high expression of C/EBP α , which was attenuated in THC-MDSC both at the transcript and protein levels. The expression of miR-690 and its target C/EBP α were inversely correlated. These results indicated that C/EBP α might be a functional target regulated by miR-690.

Regulation of C/EBP α by miR-690 was further studied by transient knockdown of the miRNA using stable antisense inhibitors with modified PNA backbone. PNA anti-miRs are a new class of modified nucleic acid antisense miRNA inhibitors that are resistant to nuclease and protease activity, thereby capable of causing sustained silencing of miRNA. In addition, they exhibit superior affinity and specificity to target RNA compared with regular DNA oligonucleotides and hence are utilized as ideal antisense reagents to inhibit miRNA effectively (35, 36). Transfection of THC-MDSCs with control anti-miR PNA did not significantly alter the expression of miR-690 as compared with mock transfection with transfection reagent alone, whereas cells transfected with anti-miR-690 PNA showed highly reduced levels of miR-690, indicating effective knockdown of the miRNA (Fig. 9F). Western blotting analysis showed markedly higher expression of C/EBP α protein in cells transfected with anti-miR-690 as compared with controls (Fig. 9, G and H), indicating unblocking and enhanced expression of C/EBP α following miR-690 knockdown. Overall, these data

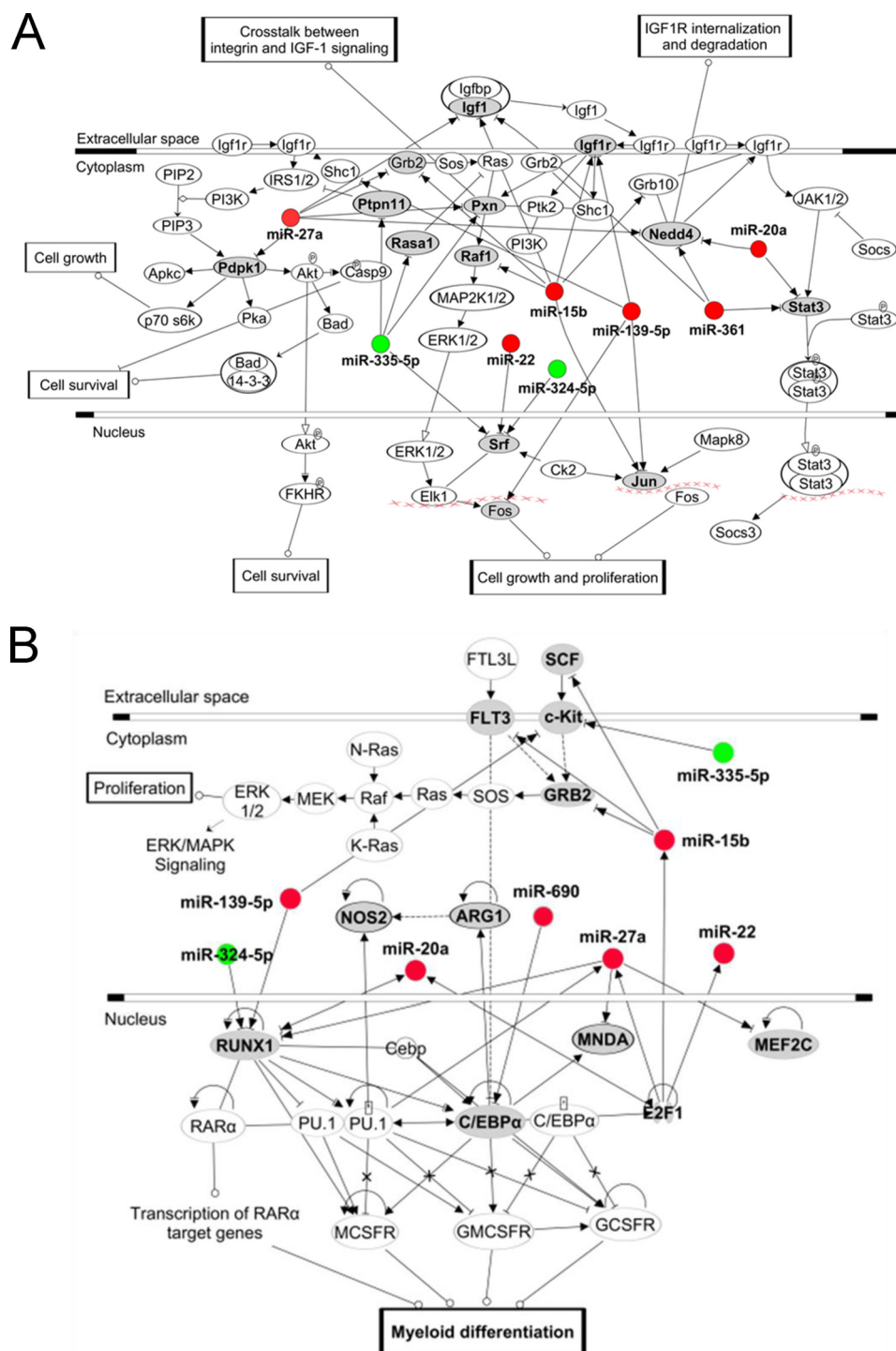


FIGURE 7. **Enriched canonical pathways of miRNA target genes.** A, IGF1 signaling pathway. The pathway map of Kyoto Encyclopedia of Genes and Genomes-derived IGF-1 signaling pathway drawn using IPA, which was the top significantly enriched canonical pathway for differentially expressed miRNA targets in THC-MDSC versus BM MDSC precursors (supplemental Table S2). B, miRNA targets were analyzed for their association with pathways involved in myeloid development, differentiation, and function using IPA. Differentially expressed miRNA in THC-MDSC are highlighted in red for overexpressed and in green for underexpressed. The direct targets of differentially expressed miRNA in the pathway are indicated in bold letters and denoted with gray ovals.

suggest that miR-690, which is relatively highly expressed in THC-induced functional MDSCs relative to its BM precursors, may play an important role by regulating and silencing C/EBP α in these cells.

To further assess the role of miR-690 and C/EBP α in MDSC subsets, we purified THC-induced CD11b⁺Ly6G⁺Ly6C⁺

granulocytic (G) and CD11b⁺Ly6G⁻Ly6C⁺ monocytic (M) subtypes by FACS sorting to >96% purity (Fig. 10, A and B) and determined their levels. Real time qPCR analysis showed marked increases in the expression of miR-690 in both subsets over control BM precursors (Fig. 10C). Moreover, C/EBP α protein expression was suppressed in both the subsets compared

TABLE 3

Important transcription factor and gene targets of differentially expressed miRNA in THC-induced MDSC

miRNA	Targets ^a
mmu-miR-690	C/ebp α
mmu-miR-22	Srf
mmu-miR-1195	Igf1, Nedd4, Stat3
mmu-miR-20a	Nedd4, Stat3 ^{b,c} , Runx1
mmu-miR-15b	Igf1, Igf1r, Jun, Raf1, Grb2, Grb10, Scf, Flt3
mmu-miR-27a	Igf1, Nedd4, Pxn, Pdpk1, Grb2, Mef2c, MNDA, Runx1 ^b
mmu-miR-139-5p	Jun, Fos, Igf1r, Shc1, c-Kit, Runx1
mmu-miR-324-5p	Srf, Runx1
mmu-miR-335-5p	Srf, Pxn, Rasa1, Ptpn11, c-Kit

^a Important targets involved in cell growth and proliferation, myeloid cell development, differentiation, and function pathways as highlighted in Fig. 7.

^b Experimentally validated miRNA targets from the curated database TarBase.

^c Experimentally validated miRNA targets from the curated database miRecords.

with BM controls (Fig. 10D). These results suggested that miR-690 is likely a pan-MDSC regulator.

To test whether miR-690 is common to MDSCs induced in response to diverse stimuli or rather unique to THC-MDSCs, we used an additional system for induction of MDSCs for comparison. We used tumor-induced MDSCs because they have been well characterized. BL/6 mice were inoculated with syngenic EL-4 tumor cells, and CD11b⁺Gr-1⁺ MDSCs from spleens of tumor-bearing mice were purified on day 14. EL-4 tumor-induced MDSCs showed a smaller yet significant increase in miR-690 over BM control (Fig. 10E). Relatively, miR-690 expression appeared to be more pronounced in THC-MDSCs.

DISCUSSION

Myeloid cells such as neutrophils, monocytes-macrophages, and dendritic cells are derived from BM marrow progenitors. Immature myeloid cells leave the BM to migrate to the periphery as they undergo differentiation and maturation. Some myeloid cells remain or get arrested in an immature state and acquire a potent functional capacity to suppress T cell responses. These are referred to as myeloid-derived suppressor cells (15, 18, 37–41). In mice, MDSCs characteristically co-express myeloid cell lineage differentiation antigen Gr-1 and CD11b (α M-integrin). CD11b⁺Gr-1⁺ cells are present in very small numbers in the spleen and periphery of naïve mice, whereas CD11b⁺Gr-1⁺ cells constitute 18–50% of normal bone marrow cells (22, 38, 42). These BM precursors are usually the primary source of MDSCs. CD11b⁺Gr-1⁺ cells from naïve BM are not immunosuppressive and need multiple signals and activation as they migrate and differentiate into functional MDSCs, at the same time their terminal differentiation is arrested so that they remain as an immature population.

MDSCs were first identified as an expanding population in response to tumors, capable of suppressing the anti-tumor immune response (37, 38, 40). MDSCs also accumulate during infectious pathologies and inflammatory conditions (39, 41, 43). Recently, we have demonstrated that natural immunosuppressive compounds such as marijuana THC can induce large numbers of CD11b⁺Gr-1⁺ functional MDSCs from bone marrow *in vivo* (22). THC-induced MDSC were found to be highly immunosuppressive capable of suppressing T cell responses *in vitro* and upon adoptive transfer *in vivo* (22).

Regulation of gene expression by miRNA is believed to be crucial in a wide range of biological processes. Emerging evidence suggests that miRNA regulate the development, differentiation, and function of a variety of immune cells including myeloid cells (8, 10, 44, 45). However, a global miRNA expression profile specific to a functional MDSC population is not known. Having made the unique observation that THC administration triggers induction of functional MDSCs (22), here we sought to investigate and compare the global miRNA expression profile of THC-MDSCs with cells of myeloid lineage to determine cell type-specific miRNA expression profile. To identify the miRNA that may be important in MDSC differentiation and function, we compared the miRNA expression between THC-MDSC and control BM precursors and identified highly differentially expressed (>2-fold) miRNA in functional THC-MDSCs. High throughput profiling was validated by real time qPCR determination of a few differentially expressed miRNA. We used a combination of computational algorithms to predict the targets of differentially expressed miRNA in functional MDSC. The miRNA targets were further analyzed for their involvement in molecular functions and pathways. We have identified several interesting and potentially important molecular interactions involved in MDSC differentiation and function.

Insulin-like growth factor (IGF1) signaling was the top canonical pathway likely influenced by target genes of differentially expressed miRNA in MDSCs induced by THC. This was particularly interesting given the fact that G-CSF was found to be a factor in the induction of MDSCs by THC (22) and was shown to have a positive effect on IGF1 signaling (46). IGF1-IGF1R signaling stimulates cell proliferation, growth, and survival in normal and malignant cells (47). Several up-regulated miRNA in THC-MDSC were found to target ubiquitin ligase Nedd4 in this pathway, which mediates IGF1R internalization and degradation. In fact, we found that Nedd4 mRNA levels were decreased in THC-MDSC. This may play a role in promoting proliferation and survival of MDSCs in periphery by enhancing IGF1R signaling. In addition, several molecules in this pathway namely, serum response factor (Srf), Ptpn11, RAS p21 protein activator 1 (Rasa1), and paxillin (Pxn) were targets of down-regulated miR-335-5p and miR-324-5p, which could influence the regulation of these targets in MDSCs by unblocking. However, Ptpn11, which was also targeted by up-regulated miRNA, was found to be down-modulated at the mRNA level in THC-MDSC.

A number of transcription factors play pivotal roles in regulating the differentiation of myeloid cells into active mediators of the innate immune system. Several among them, namely PU.1, RUNX1, C/EBP α , and c-JUN, were found to be the direct targets of differentially expressed miRNA in THC-MDSC. Extensive cross-talk between these transcription factors is further known to control complex pathways of monocytic and granulocytic differentiation (48). Runx1 stimulates proliferation and differentiation of myeloid progenitors (49). Multiple overexpressed and underexpressed miRNA in THC-MDSC had good binding sites on *Runx1* mRNA 3'-UTR, which indicated a typically complex, probably finely tuned miRNA regulatory circuit. Among these, miR-27-Runx1 was noted to be

miRNA Expression Profiling of THC-induced Functional MDSCs

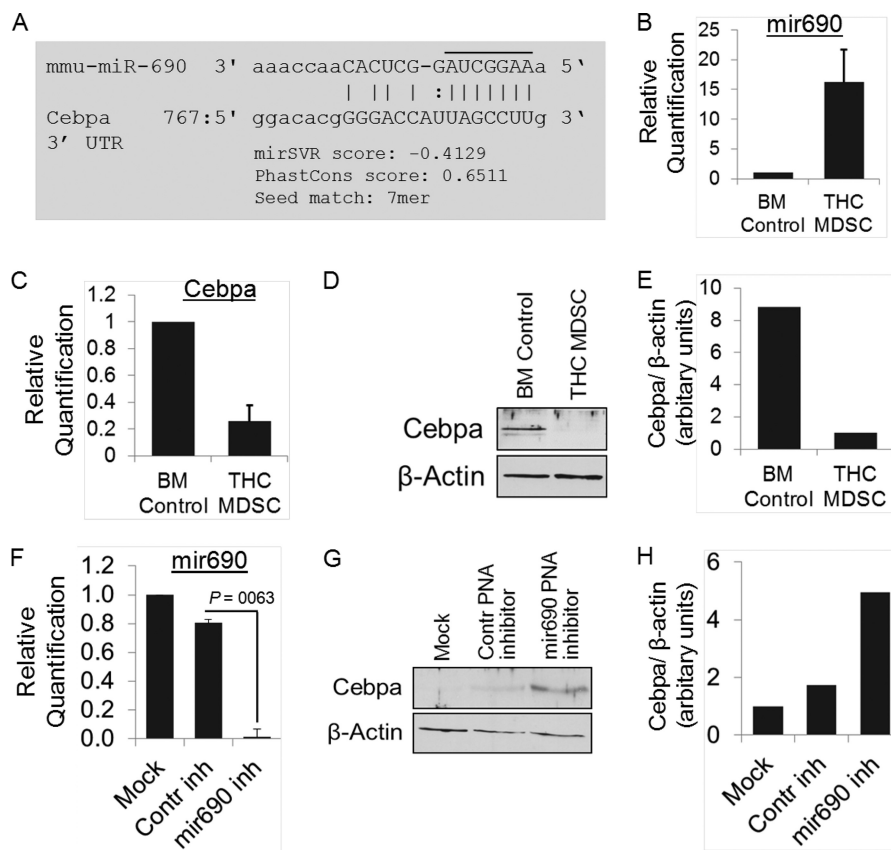


FIGURE 9. Regulation of C/EBP α by miR-690 in MDSCs. *A*, target prediction of mmu-miR-690 using miRanda-mirSVR and TargetScanS showing alignment of mature miRNA with 3'-UTR of *C/ebp α* mRNA. miR-690-binding site with 7-mer-m8 seed match (an exact match to positions 2–8 of the mature miRNA (the seed + position 8)) resides at nucleotide positions 782–788 of *C/ebp α* mRNA 3'-UTR. *B*, real time qPCR determination of miR-690 normalized to endogenous control U6 in BM precursors and THC-MDSC. *C*, real time qPCR analysis of *C/ebp α* mRNA in THC-MDSC versus BM precursors normalized to 18 S. *D*, Western blotting analysis of C/EBP α protein expression. *E*, densitometry of Western blotting showing relative expression of C/EBP α normalized to control β -actin. *F* and *G*, total RNA was extracted from THC-MDSCs transfected with negative control PNA anti-miR or PNA anti-miR-690 (500 nmol/liter) in the presence of Lipofectamine 2000 reagent. *F*, miR-690 expression analyzed by real time qPCR and normalized to U6 shows effective knockdown of miRNA-690 in THC-MDSC. *G*, analysis of C/EBP α by Western blotting following miR-690 knockdown in THC-MDSC. *H*, relative expression normalized to control β -actin as determined by densitometry. *inh*, inhibitor.

The E2F family of transcription factors can enhance the expression of a number of miRNA, for example miR-15b, miR-20a, miR-22, and miR-27a, likely by directly binding to the promoters and activating their transcription (50, 51). Interestingly, E2f1 was increased, and all these miRNA were overexpressed in THC-induced MDSCs.

It is an exciting and major finding that miR-690, highly overexpressed in THC-MDSC relative to control BM-MDSC precursors, targets C/EBP α . C/EBP α is an important transcription factor involved in the development of granulocyte-monocyte progenitors and their subsequent terminal differentiation (52, 53). *C/ebp α* ^(-/-) null mice lack mature granulocytes (54); activation of C/EBP α in mice expressing its inducible form leads to increases in mature granulocytes and myeloid progenitors (55). These studies demonstrate the critical nature of C/EBP α in the terminal differentiation granulocytes. We observed higher expression of C/EBP α in BM MDSC precursors and attenuated levels in THC-MDSCs, with a reciprocal relationship with miR-690 expression. We further established the functional link between these two by inhibiting miR-690 in THC-MDSCs, which appeared to unblock leading to significant up-regulation of C/EBP α . Regulation of some E2F family proteins by C/EBP α plays a role in its ability to induce terminal granulocyte differ-

entiation (56). Master transcription factor PU.1 regulates macrophage differentiation (57), and interaction of PU.1 with C/EBP α contributes to this process (52). We have shown here as well as previously (22) that THC induces both granulocytic and monocytic MDSC subsets. Furthermore, C/EBP α is also known to block cell cycle progression by interacting with E2F proteins so that a loss of C/EBP α leads to increased myeloid proliferation (58). We have seen significant proliferation of THC-induced MDSCs *in vivo* in the periphery (22), further demonstrated here by Ki67 staining. This, coupled with the detection of immature myeloid marker CD31, supports the hypothesis that they are derived from BM precursors and arrested at an immature state acquiring potent suppressive activity. These observations also rule out the possibility of reprogramming of mature myeloid cells into suppressor cells by THC. Both MDSC subsets induced by THC express high levels of miR-690 with attenuated C/EBP α expression. Moreover, a smaller but significant increase in miR-690 expression could be seen in tumor-induced MDSCs. Therefore, we propose here that up-regulation of miR-690 and silencing of C/EBP α play crucial roles during the development of functional MDSC in general, by blocking or slowing their terminal differentiation

miRNA Expression Profiling of THC-induced Functional MDSCs

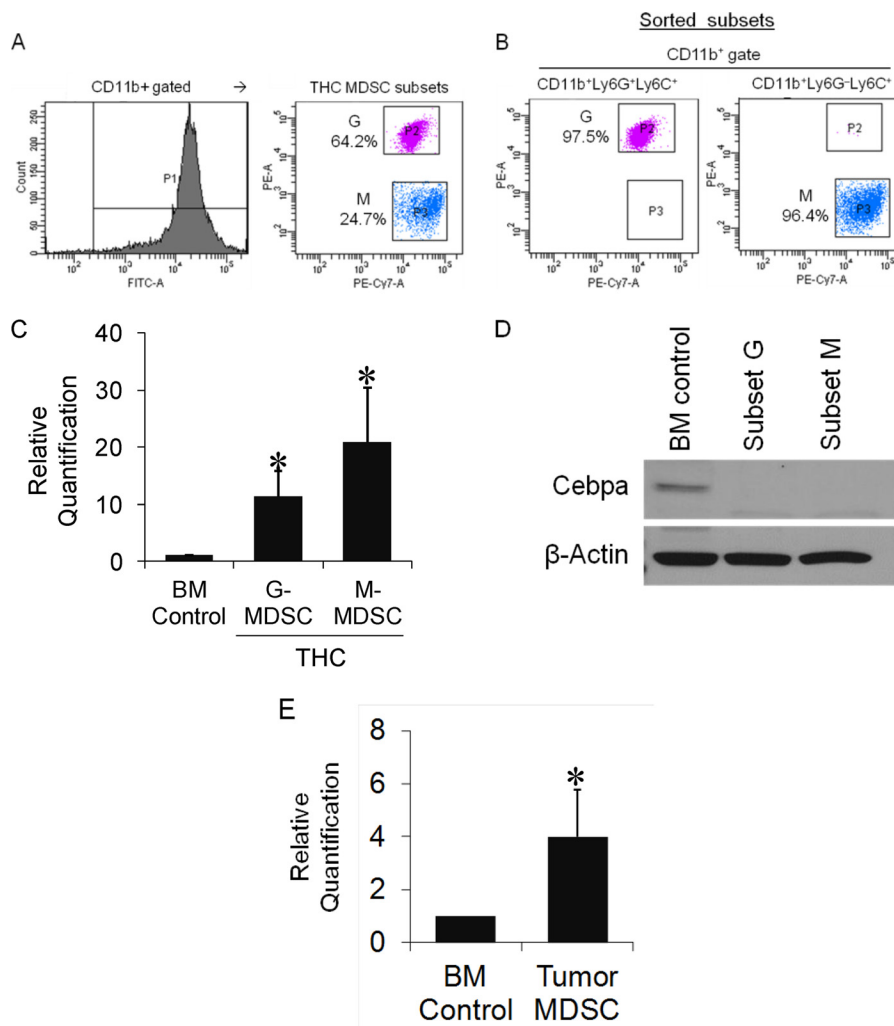


FIGURE 10. Determination of miR-690 and C/EBP α in MDSC subsets. *A* and *B*, MDSCs harvested from the peritoneum of THC-injected mice were triple stained and FACS sorted for CD11b⁺Ly6G⁺Ly6C⁺ and CD11b⁺Ly6G⁻Ly6C⁺ subsets to >96% purity and used for extraction of total RNA and protein. *C* and *D*, miR-690 levels were determined by real time qPCR and normalized to control miRNA U6 (*C*) and C/EBP α protein expression by Western blotting (*D*). *E*, analysis of miR-690 in tumor-induced MDSCs. CD11b⁺Gr-1⁺ MDSCs from spleens EL-4 tumor-bearing mice were purified by sorting, and total RNA was extracted. miR-690 levels were determined by qPCR and normalized to U6 and compared with control BM precursors. *, $p < 0.05$ compared with BM control.

while maintaining the immature immunosuppressive state at the same time aiding their proliferation.

A few studies have explored the role of specific miRNA associated with development of MDSCs recently, particularly in tumor models (59–62). miR-223 was reported to suppress the accumulation of BM-derived MDSCs (59). However, it is inconclusive, because in another study, miR-223 null mice were found to exhibit enhanced, hypermature neutrophilic phenotype (60). Further, miR-223 was found to negatively regulate progenitor proliferation, granulocyte differentiation, and activation in a MEF2C-dependent manner (60). miR-494 expression induced by tumor-derived TGF- β 1 was shown to play a critical role in the regulation of accumulation and function of tumor-expanded MDSCs by specifically targeting PTEN (61). miR-17-5p and miR-20a could decrease the expression of reactive oxygen species and suppressive function of tumor-induced MDSCs by targeting Stat3 (62). In the current study, miR-223, miR-494, and miR-17-5p expression levels were <2-fold between THC-MDSCs and BM precursors and hence not significantly altered, whereas miR-20a was found to be up-regu-

lated, suggesting possible unique differences between tumor-induced and THC-induced MDSC with regards to miRNA regulatory circuits. It should be noted that tumor-induced expansion of MDSCs involves tumor-derived factors such as IL-1 β , IL-6, TGF- β 1, S100 proteins, prostaglandin E2, or various cytokines and chemokines such as CXCL12 (SDF1) and G-CSF (16, 63–65), whereas expansion of MDSCs in response to THC was found to be primarily mediated by G-CSF in association with CXCL1 (22).

In this report, we have presented the miRNA expression profile of CD11b⁺Gr-1⁺ functional MDSCs induced by the immunosuppressive cannabinoid THC *in vivo*. We have identified the select set of differentially expressed miRNA in functional MDSCs that are significantly altered when compared with their BM precursors. We have identified several interesting miRNA-target interactions involved in cell growth and proliferation and myeloid differentiation with potential functional role in MDSC development, expansion, and function. Distinct miRNA expression in MDSCs also highlights how unique they are compared with various other myeloid cells with respect to molecu-

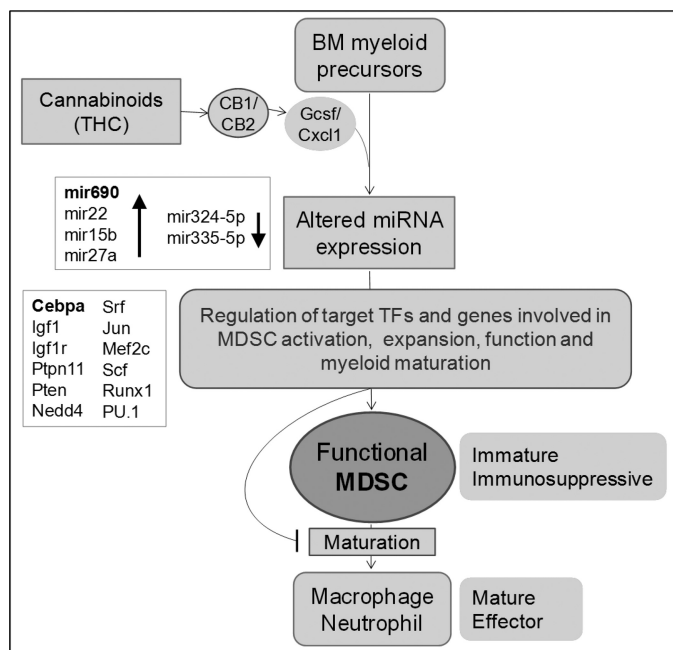


FIGURE 11. Schematic representation of proposed involvement of miRNA and their target genes in the induction of functional MDSC from bone marrow. We have previously shown that induction of functional MDSCs by THC *in vivo* is dependent on cannabinoid receptor activation and is primarily mediated by G-CSF and CXCL1 chemokines (22). Here we demonstrate distinct, altered miRNA expression profile of THC-induced functional MDSCs relative to BM precursors. We propose that select miRNA play important roles in the generation of functional MDSC by targeting and regulating crucial transcription factors, genes, and pathways involved in MDSC generation, expansion, and function. Moreover, miRNA may be crucial in the arrest of MDSCs in an immature state by negatively regulating genes involved in their terminal differentiation into mature granulocytes and macrophages.

lar signatures. Our conclusions and proposed mechanisms are presented in a schematic summary (Fig. 11). miRNA expression profiling and pathway analysis of target genes leads us to conclude that miRNA may play a crucial role in the generation of functional MDSCs by regulating several important transcription factors and target genes, thereby promoting myeloid differentiation, MDSC expansion, and function, at the same time blocking their terminal maturation. Select differentially expressed miRNA such as miR-690, which appears to regulate C/EBP α as identified here, will be attractive molecular targets to manipulate MDSC activity in inflammatory diseases as well as cancer.

REFERENCES

1. Pasquinelli, A. E. (2012) MicroRNAs and their targets. Recognition, regulation and an emerging reciprocal relationship. *Nat. Rev. Genet.* **13**, 271–282
2. Grimson, A., Farh, K. K., Johnston, W. K., Garrett-Engele, P., Lim, L. P., and Bartel, D. P. (2007) MicroRNA targeting specificity in mammals. Determinants beyond seed pairing. *Mol. Cell* **27**, 91–105
3. Bartel, D. P. (2009) MicroRNAs. Target recognition and regulatory functions. *Cell* **136**, 215–233
4. Friedman, R. C., Farh, K. K., Burge, C. B., and Bartel, D. P. (2009) Most mammalian mRNAs are conserved targets of microRNAs. *Genome Res.* **19**, 92–105
5. Landgraf, P., Rusu, M., Sheridan, R., Sewer, A., Iovino, N., Aravin, A., Pfeffer, S., Rice, A., Kamphorst, A. O., Landthaler, M., Lin, C., Socci, N. D., Hermida, L., Fulci, V., Chiaretti, S., Foà, R., Schliwka, J., Fuchs, U., Novosel, A., Müller, R.-U., Schermer, B., Bissels, U., Inman, J., Phan, Q., Chien, M., Weir, D. B., Choksi, R., De Vita, G., Frezzetti, D., Trompeter, H.-I., Hor-

- nung, V., Teng, G., Hartmann, G., Palkovits, M., Di Lauro, R., Wernet, P., Macino, G., Rogler, C. E., Nagle, J. W., Ju, J., Papavasiliou, F. N., Benzing, T., Lichter, P., Tam, W., Brownstein, M. J., Bosio, A., Borkhardt, A., Russo, J. J., Sander, C., Zavolan, M., and Tuschl, T. (2007) A mammalian microRNA expression atlas based on small RNA library sequencing. *Cell* **129**, 1401–1414
6. Guan, H., Fan, D., Mrelashvili, D., Hao, H., Singh, N. P., Singh, U. P., Nagarkatti, P. S., and Nagarkatti, M. (2013) MicroRNA let-7e is associated with the pathogenesis of experimental autoimmune encephalomyelitis. *Eur. J. Immunol.* **43**, 104–114
7. Singh, N. P., Singh, U. P., Guan, H., Nagarkatti, P., and Nagarkatti, M. (2012) Prenatal exposure to TCDD triggers significant modulation of microRNA expression profile in the thymus that affects consequent gene expression. *PLoS One* **7**, e45054
8. O’Connell, R. M., Rao, D. S., Chaudhuri, A. A., and Baltimore, D. (2010) Physiological and pathological roles for microRNAs in the immune system. *Nat. Rev. Immunol.* **10**, 111–122
9. Rossi, R. L., Rossetti, G., Wenandy, L., Curti, S., Ripamonti, A., Bonnal, R. J., Birolo, R. S., Moro, M., Crosti, M. C., Gruarin, P., Maglie, S., Marabita, F., Mascheroni, D., Parente, V., Comelli, M., Trabucchi, E., De Francesco, R., Geginat, J., Abrignani, S., and Pagani, M. (2011) Distinct microRNA signatures in human lymphocyte subsets and enforcement of the naive state in CD4⁺ T cells by the microRNA miR-125b. *Nat. Immunol.* **12**, 796–803
10. Neilson, J. R., Zheng, G. X., Burge, C. B., and Sharp, P. A. (2007) Dynamic regulation of miRNA expression in ordered stages of cellular development. *Genes Dev.* **21**, 578–589
11. Kuchen, S., Resch, W., Yamane, A., Kuo, N., Li, Z., Chakraborty, T., Wei, L., Laurence, A., Yasuda, T., Peng, S., Hu-Li, J., Lu, K., Dubois, W., Kitamura, Y., Charles, N., Sun, H. W., Muljo, S., Schwartzberg, P. L., Paul, W. E., O’Shea, J., Rajewsky, K., and Casellas, R. (2010) Regulation of microRNA expression and abundance during lymphopoiesis. *Immunity* **32**, 828–839
12. Monticelli, S., Ansel, K. M., Xiao, C., Socci, N. D., Krichevsky, A. M., Thai, T.-H., Rajewsky, N., Marks, D. S., Sander, C., Rajewsky, K., Rao, A., and Kosik, K. S. (2005) MicroRNA profiling of the murine hematopoietic system. *Genome Biol.* **6**, R71
13. Waight, J. D., Netherby, C., Hensen, M. L., Miller, A., Hu, Q., Liu, S., Bogner, P. N., Farren, M. R., Lee, K. P., Liu, K., and Abrams, S. I. (2013) Myeloid-derived suppressor cell development is regulated by a STAT/IRF-8 axis. *J. Clin. Invest.* **123**, 4464–4478
14. Xia, S., Sha, H., Yang, L., Ji, Y., Ostrand-Rosenberg, S., and Qi, L. (2011) Gr-1⁺ CD11b⁺ myeloid-derived suppressor cells suppress inflammation and promote insulin sensitivity in obesity. *J. Biol. Chem.* **286**, 23591–23599
15. Gabrilovich, D. I., and Nagaraj, S. (2009) Myeloid-derived suppressor cells as regulators of the immune system. *Nat. Rev. Immunol.* **9**, 162–174
16. Ostrand-Rosenberg, S., and Sinha, P. (2009) Myeloid-derived suppressor cells. Linking inflammation and cancer. *J. Immunol.* **182**, 4499–4506
17. Lees, J. R., Azimzadeh, A. M., and Bromberg, J. S. (2011) Myeloid derived suppressor cells in transplantation. *Curr. Opin. Immunol.* **23**, 692–697
18. Bronte, V., Serafini, P., Mazzoni, A., Segal, D. M., and Zanovello, P. (2003) L-arginine metabolism in myeloid cells controls T-lymphocyte functions. *Trends Immunol.* **24**, 302–306
19. Singh, U. P., Singh, N. P., Singh, B., Hofseth, L. J., Taub, D. D., Price, R. L., Nagarkatti, M., and Nagarkatti, P. S. (2012) Role of resveratrol-induced CD11b⁺ Gr-1⁺ myeloid derived suppressor cells (MDSCs) in the reduction of CXCR3⁺ T cells and amelioration of chronic colitis in IL-10^{-/-} mice. *Brain Behav. Immun.* **26**, 72–82
20. Rieder, S. A., Nagarkatti, P., and Nagarkatti, M. (2012) Multiple anti-inflammatory pathways triggered by resveratrol lead to amelioration of staphylococcal enterotoxin B-induced lung injury. *Br. J. Pharmacol.* **167**, 1244–1258
21. Guan, H., Singh, N. P., Singh, U. P., Nagarkatti, P. S., and Nagarkatti, M. (2012) Resveratrol prevents endothelial cells injury in high-dose interleukin-2 therapy against melanoma. *PLoS One* **7**, e35650
22. Hegde, V. L., Nagarkatti, M., and Nagarkatti, P. S. (2010) Cannabinoid receptor activation leads to massive mobilization of myeloid-derived sup-

- pressor cells with potent immunosuppressive properties. *Eur. J. Immunol.* **40**, 3358–3371
23. Hegde, V. L., Nagarkatti, P. S., and Nagarkatti, M. (2011) Role of myeloid-derived suppressor cells in amelioration of experimental autoimmune hepatitis following activation of TRPV1 receptors by cannabidiol. *PLoS One* **6**, e18281
 24. Juhila, J., Sipilä, T., Icaý, K., Nicorici, D., Ellonen, P., Kallio, A., Korpeinen, E., Greco, D., and Hovatta, I. (2011) MicroRNA expression profiling reveals miRNA families regulating specific biological pathways in mouse frontal cortex and hippocampus. *PLoS One* **6**, e21495
 25. Kozomara, A., and Griffiths-Jones, S. (2011) miRBase. Integrating microRNA annotation and deep-sequencing data. *Nucleic Acids Res.* **39**, D152–D157
 26. Rehmsmeier, M., Steffen, P., Hochsmann, M., and Giegerich, R. (2004) Fast and effective prediction of microRNA/target duplexes. *RNA* **10**, 1507–1517
 27. Betel, D., Koppal, A., Agius, P., Sander, C., and Leslie, C. (2010) Comprehensive modeling of microRNA targets predicts functional non-conserved and non-canonical sites. *Genome Biol.* **11**, R90
 28. Dweep, H., Sticht, C., Pandey, P., and Gretz, N. (2011) miRWalk database. Prediction of possible miRNA binding sites by “walking” the genes of three genomes. *J. Biomed. Inform.* **44**, 839–847
 29. Xiao, F., Zuo, Z., Cai, G., Kang, S., Gao, X., and Li, T. (2009) miRecords. An integrated resource for microRNA–target interactions. *Nucleic Acids Res.* **37**, D105–D110
 30. Vergoulis, T., Vlachos, I. S., Alexiou, P., Georgakilas, G., Maragkakias, M., Reczko, M., Gerangelos, S., Koziris, N., Dalamagas, T., and Hatzigeorgiou, A. G. (2012) TarBase 6.0. Capturing the exponential growth of miRNA targets with experimental support. *Nucleic Acids Res.* **40**, D222–D229
 31. Kanehisa, M., Goto, S., Sato, Y., Furumichi, M., and Tanabe, M. (2012) KEGG for integration and interpretation of large-scale molecular data sets. *Nucleic Acids Res.* **40**, D109–D114
 32. Cline, M. S., Smoot, M., Cerami, E., Kuchinsky, A., Landys, N., Workman, C., Christmas, R., Avila-Campilo, I., Creech, M., Gross, B., Hanspers, K., Isserlin, R., Kelley, R., Killcoyne, S., Lotia, S., Maere, S., Morris, J., Ono, K., Pavlovic, V., Pico, A. R., Vailaya, A., Wang, P.-L., Adler, A., Conklin, B. R., Hood, L., Kuiper, M., Sander, C., Schmulevich, I., Schwikowski, B., Warner, G. J., Ideker, T., and Bader, G. D. (2007) Integration of biological networks and gene expression data using Cytoscape. *Nat. Protoc.* **2**, 2366–2382
 33. Bindea, G., Mlecnik, B., Hackl, H., Charoentong, P., Tosolini, M., Kirilovsky, A., Fridman, W.-H., Pagès, F., Trajanoski, Z., and Galon, J. (2009) ClueGO. A Cytoscape plug-in to decipher functionally grouped gene ontology and pathway annotation networks. *Bioinformatics* **25**, 1091–1093
 34. Pang, K. C., Frith, M. C., and Mattick, J. S. (2006) Rapid evolution of noncoding RNAs. Lack of conservation does not mean lack of function. *Trends Genet.* **22**, 1–5
 35. Oh, S. Y., Ju, Y., and Park, H. (2009) A highly effective and long-lasting inhibition of miRNAs with PNA-based antisense oligonucleotides. *Mol. Cells* **28**, 341–345
 36. Fabbri, E., Manicardi, A., Tedeschi, T., Sforza, S., Bianchi, N., Brognara, E., Finotti, A., Breveglieri, G., Borgatti, M., Corradini, R., Marchelli, R., and Gambari, R. (2011) Modulation of the biological activity of microRNA-210 with peptide nucleic acids (PNAs). *ChemMedChem* **6**, 2192–2202
 37. Kuzmartsev, S., and Gabrilovich, D. I. (2002) Immature myeloid cells and cancer-associated immune suppression. *Cancer Immunol. Immunother.* **51**, 293–298
 38. Bronte, V., Apolloni, E., Cabrelle, A., Ronca, R., Serafini, P., Zamboni, P., Restifo, N. P., and Zanoello, P. (2000) Identification of a CD11b⁺/Gr-1⁺/CD31⁺ myeloid progenitor capable of activating or suppressing CD8⁺ T cells. *Blood* **96**, 3838–3846
 39. Delano, M. J., Scumpia, P. O., Weinstein, J. S., Coco, D., Nagaraj, S., Kelly-Scumpia, K. M., O'Malley, K. A., Wynn, J. L., Antonenko, S., Al-Quran, S. Z., Swan, R., Chung, C.-S., Atkinson, M. A., Ramphal, R., Gabrilovich, D. I., Reeves, W. H., Ayala, A., Phillips, J., Laface, D., Heyworth, P. G., Clare-Salzler, M., and Moldawer, L. L. (2007) MyD88-dependent expansion of an immature GR-1⁺CD11b⁺ population induces T cell suppression and Th2 polarization in sepsis. *J. Exp. Med.* **204**, 1463–1474
 40. Li, Q., Pan, P.-Y., Gu, P., Xu, D., and Chen, S.-H. (2004) Role of immature myeloid Gr-1⁺ cells in the development of antitumor immunity. *Cancer Res.* **64**, 1130–1139
 41. Goñi, O., Alcaide, P., and Fresno, M. (2002) Immunosuppression during acute *Trypanosoma cruzi* infection. Involvement of Ly6G (Gr1⁺)CD11b⁺ immature myeloid suppressor cells. *Int. Immunol.* **14**, 1125–1134
 42. Hock, H., Hamblen, M. J., Rooke, H. M., Traver, D., Bronson, R. T., Cameron, S., and Orkin, S. H. (2003) Intrinsic requirement for zinc finger transcription factor Gfi-1 in neutrophil differentiation. *Immunity* **18**, 109–120
 43. Haile, L. A., von Wasielewski, R., Gamrekeshvili, J., Krüger, C., Bachmann, O., Westendorf, A. M., Buer, J., Liblau, R., Manns, M. P., Korangy, F., and Greten, T. F. (2008) Myeloid-derived suppressor cells in inflammatory bowel disease. A new immunoregulatory pathway. *Gastroenterology* **135**, 871–881, 881.e1–5
 44. O'Connell, R. M., Zhao, J. L., and Rao, D. S. (2011) MicroRNA function in myeloid biology. *Blood* **118**, 2960–2969
 45. Yang, G., Yang, L., Zhao, Z., Wang, J., and Zhang, X. (2012) Signature miRNAs involved in the innate immunity of invertebrates. *PLoS One* **7**, e39015
 46. Arkins, S., Rebeiz, N., Brunke-Reese, D. L., Minshall, C., and Kelley, K. W. (1995) The colony-stimulating factors induce expression of insulin-like growth factor-I messenger ribonucleic acid during hematopoiesis. *Endocrinology* **136**, 1153–1160
 47. Vincent, A. M., and Feldman, E. L. (2002) Control of cell survival by IGF signaling pathways. *Growth Horm. IGF Res.* **12**, 193–197
 48. Rosenbauer, F., and Tenen, D. G. (2007) Transcription factors in myeloid development. Balancing differentiation with transformation. *Nat. Rev. Immunol.* **7**, 105–117
 49. Friedman, A. D. (2002) Runx1, c-Myb, and C/EBP α couple differentiation to proliferation or growth arrest during hematopoiesis. *J. Cell. Biochem.* **86**, 624–629
 50. Sylvestre, Y., De Guire, V., Querido, E., Mukhopadhyay, U. K., Bourdeau, V., Major, F., Ferbeyre, G., and Chartrand, P. (2007) An E2F/miR-20a autoregulatory feedback loop. *J. Biol. Chem.* **282**, 2135–2143
 51. Bueno, M. J., Gómez de Cedrón, M., Laresgoiti, U., Fernández-Piqueras, J., Zubiaga, A. M., and Malumbres, M. (2010) Multiple E2F-induced microRNAs prevent replicative stress in response to mitogenic signaling. *Mol. Cell Biol.* **30**, 2983–2995
 52. Wang, D., D'Costa, J., Civin, C. I., and Friedman, A. D. (2006) C/EBP α directs monocytic commitment of primary myeloid progenitors. *Blood* **108**, 1223–1229
 53. Collins, S. J., Ulmer, J., Purton, L. E., and Darlington, G. (2001) Multipotent hematopoietic cell lines derived from C/EBP α ^{-/-} knockout mice display granulocyte macrophage–colony-stimulating factor, granulocyte–colony-stimulating factor, and retinoic acid-induced granulocytic differentiation. *Blood* **98**, 2382–2388
 54. Zhang, D. E., Zhang, P., Wang, N. D., Hetherington, C. J., Darlington, G. J., and Tenen, D. G. (1997) Absence of granulocyte colony-stimulating factor signaling and neutrophil development in CCAAT enhancer binding protein α -deficient mice. *Proc. Natl. Acad. Sci. U.S.A.* **94**, 569–574
 55. Fukuchi, Y., Shibata, F., Ito, M., Goto-Koshino, Y., Sotomaru, Y., Ito, M., Kitamura, T., and Nakajima, H. (2006) Comprehensive analysis of myeloid lineage conversion using mice expressing an inducible form of C/EBP α . *EMBO J.* **25**, 3398–3410
 56. D'Alo, F., Johansen, L. M., Nelson, E. A., Radomska, H. S., Evans, E. K., Zhang, P., Nerlov, C., and Tenen, D. G. (2003) The amino terminal and E2F interaction domains are critical for C/EBP α -mediated induction of granulopoietic development of hematopoietic cells. *Blood* **102**, 3163–3171
 57. DeKoter, R. P., Walsh, J. C., and Singh, H. (1998) PU. 1 regulates both cytokine-dependent proliferation and differentiation of granulocyte/macrophage progenitors. *EMBO J.* **17**, 4456–4468
 58. Porse, B. T., Bryder, D., Theilgaard-Mönch, K., Hasemann, M. S., Anderson, K., Damgaard, I., Jacobsen, S. E., and Nerlov, C. (2005) Loss of C/EBP α cell cycle control increases myeloid progenitor proliferation and transforms the neutrophil granulocyte lineage. *J. Exp. Med.* **202**, 85–96
 59. Liu, Q., Zhang, M., Jiang, X., Zhang, Z., Dai, L., Min, S., Wu, X., He, Q., Liu,

miRNA Expression Profiling of THC-induced Functional MDSCs

- J., Zhang, Y., Zhang, Z., and Yang, R. (2011) miR-223 suppresses differentiation of tumor-induced CD11b⁺ Gr1⁺ myeloid-derived suppressor cells from bone marrow cells. *Int. J. Cancer* **129**, 2662–2673
60. Johnnidis, J. B., Harris, M. H., Wheeler, R. T., Stehling-Sun, S., Lam, M. H., Kirak, O., Brummelkamp, T. R., Fleming, M. D., and Camargo, F. D. (2008) Regulation of progenitor cell proliferation and granulocyte function by microRNA-223. *Nature* **451**, 1125–1129
61. Liu, Y., Lai, L., Chen, Q., Song, Y., Xu, S., Ma, F., Wang, X., Wang, J., Yu, H., Cao, X., and Wang, Q. (2012) MicroRNA-494 is required for the accumulation and functions of tumor-expanded myeloid-derived suppressor cells via targeting of PTEN. *J. Immunol.* **188**, 5500–5510
62. Zhang, M., Liu, Q., Mi, S., Liang, X., Zhang, Z., Su, X., Liu, J., Chen, Y., Wang, M., Zhang, Y., Guo, F., Zhang, Z., and Yang, R. (2011) Both miR-17-5p and miR-20a alleviate suppressive potential of myeloid-derived suppressor cells by modulating STAT3 expression. *J. Immunol.* **186**, 4716–4724
63. Sinha, P., Okoro, C., Foell, D., Freeze, H. H., Ostrand-Rosenberg, S., and Srikrishna, G. (2008) Proinflammatory S100 proteins regulate the accumulation of myeloid-derived suppressor cells. *J. Immunol.* **181**, 4666–4675
64. Xiang, X., Poliakov, A., Liu, C., Liu, Y., Deng, Z. B., Wang, J., Cheng, Z., Shah, S. V., Wang, G.-J., Zhang, L., Grizzle, W. E., Mobley, J., and Zhang, H.-G. (2009) Induction of myeloid-derived suppressor cells by tumor exosomes. *Int. J. Cancer* **124**, 2621–2633
65. Obermajer, N., Muthuswamy, R., Odunsi, K., Edwards, R. P., and Kalinski, P. (2011) PGE₂-induced CXCL12 production and CXCR4 expression controls the accumulation of human MDSCs in ovarian cancer environment. *Cancer Res.* **71**, 7463–7470